The Relationship between Area–Time Integrals Determined from Satellite Infrared Data by Means of a Fixed-Threshold Approach and Convective Rainfall Volumes

L. RONALD JOHNSON AND PAUL L. SMITH

Institute of Atmospheric Sciences, South Dakota School of Mines and Technology, Rapid City, South Dakota

THOMAS H. VONDER HAAR AND DONALD REINKE

Cooperative Institute for Research in the Atmosphere, Colorado State University, Fort Collins, Colorado

(Manuscript received 29 March 1993, in final form 1 September 1993)

ABSTRACT

The relationship of the rainfall from convective clouds to area–time integrals determined from satellite infrared data using a fixed infrared-temperature threshold is investigated. Concurrent radar and rapid-scan satellite data obtained during field projects in the northern High Plains and the southeastern United States were used in this study. The fixed IR threshold appropriate for each region was determined by an optimization procedure that identified the brightness threshold that yields the strongest relationship between estimated rainfall from a cloud cluster and its satellite area–time integral (ATI) for each dataset. For the North Dakota–Montana area the optimization procedure indicated that the area enclosed by the −22.5°C isotherm provides satellite ATI values most closely related to the estimated rainfalls. For the southeastern United States project, the optimized temperature threshold was 8.5°C. The difference between the thresholds determined for the two geographic areas suggests that a different "calibration" for each distinct area may be needed to make use of this relationship. Slopes of the two log–log rainfall–ATI regressions are less than unity, indicating that a relative horizontal expansion and/or increase in persistence of a cloud cluster exceeds the associated increase in precipitation. Implications for the Geostationary Operational Environmental Satellite precipitation index are discussed. New results concerning the rain volume–radar ATI relationship for the southeastern United States are also appended to the paper.

1. Introduction

The volume of rain produced by convective clouds is obviously related in some way to their areal extent and their lifetime. This has been recognized in a quantitative way at least since the work of Byers (1948). The explicit formulation of this relationship that shows the strongest correlation appears to be the radar rain volume/area–time integral relationship introduced in Doneaud et al. (1981, 1984b) and since discussed by Lopez et al. (1989), Atlas et al. (1990), and others.

The area–time integral (ATI) concept derives from the basic expression for the rain volume V produced by any cloud entity:

$$V = \int_t \int_a R(\mathbf{r}, t)\,da\,dt. \qquad (1)$$

Here $R(\mathbf{r}, t)$ represents the rainfall rate, variable in space and time, while da and dt represent increments of area and time, and a, t denote the area–time domain of interest. The area a can be specified with respect to either the cloud itself (a "floating-target" viewpoint) or some given area on the surface (a "fixed-target" view). According to the mean value theorem, (1) may be rewritten as

$$V = \bar{R} \int_t \int_a da\,dt, \qquad (2)$$

with $\bar{R}$ representing the mean rainfall rate over the area–time domain involved. If the limits of integration are extended to encompass the entire areal extent A and duration T of a convective entity, the integral in (2) becomes the ATI.

The ATI calculation is usually considered to involve only the rainy area(s) and time period(s), but this is not an inherent requirement; incorporating areas or time periods without rain into (1) does not affect the end result. Such incorporation will, of course, affect the numerical value of the ATI and the associated value of $\bar{R}$ in (2); that may or may not affect the correlation between V and the ATI appreciably.

With radar data, more direct means of deriving rainfall estimates are available. Furthermore, the geograph-

Corresponding author address: L. Ronald Johnson, Institute of Atmospheric Sciences, South Dakota School of Mines and Technology, 501 E. St. Joseph Street, Rapid City, SD 57701-3995.

ical coverage of weather radar (while expanding) is quite limited and probably will never extend to oceanic areas of the globe. Thus, satellite-based methods of deriving rainfall estimates assume considerable importance for many applications (e.g., Barrett and Martin 1981; Arkin and Ardanuy 1989). One important method of deriving such estimates is the Geostationary Operational Environmental Satellite (GOES) precipitation index (GPI) introduced by Arkin and Meisner (1987). Atlas and Bell (1992) have recently pointed out that the GPI is, in fact, a kind of area–time integral (employing the fixed-target point of view). Indeed, the possibility of an ATI-type relationship is implicit in the early work of Stout et al. (1979) on satellite rainfall estimation. They described the volumetric rainfall rate R_v from a convective cloud by the expression

$$R_v = a_0 A + a_1 \frac{dA}{dt}, \tag{3}$$

with a_0 and a_1 being empirical constants. Integration of this expression over the cloud lifetime leads directly to

$$V = a_0 \int_0^T A dt. \tag{4}$$

This integral is just the satellite area–time integral (SATI), and following Doneaud et al. (1984a), the factor a_0 can be recognized as the mean rainfall rate. According to the Stout et al. analysis, the value of a_0 should be independent of the size and duration of the cloud, but the results herein provide a different indication.

The variations in the rainfall and the cloud area are generally out of synchronism, as noted by Stout et al. (1979), and the cloud area generally exceeds the associated rain area, as noted by Atlas and Bell (1992). A satellite view can readily determine the area of cloud cover but it is very difficult to determine the rainy area within; much effort has been devoted to this (e.g., Griffith et al. 1978; Scofield 1987; Adler and Negri 1988; Tsonis 1988), with rather limited success except for those events with very high rain rates. It is therefore not generally possible to localize the rainfall in either space or time within the footprint of the cloud from an SATI calculation. However, for many purposes such as storm water budgets and regional or continental scale analyses, such localization may not actually be necessary.

Following the success with the radar ATI analysis, Doneaud et al. (1987) launched an investigation to determine whether a similar relationship could be identified between rain volume and the SATI. They again adopted the floating-target point of view and dealt with cloud clusters that could be isolated fairly easily rather than try to pick out individual cloud elements within such clusters. Their preliminary results indicated that some relationship of this kind exists, but the sample was quite small and further investigation was called for. This paper reports on the part of that extended investigation in which the infrared threshold used to define the cloud area for SATI calculations for a given geographic location is held fixed. The results, however, suggest a need for different thresholds for locations with differing dominant precipitation mechanisms.

2. Analysis of data collected during CCOPE and NDCMP projects

Radar surveillance scans correlated with rapid-scan infrared data obtained by a GOES satellite provide the necessary ingredients for this study. Radar and GOES rapid-scan data were collected from the northern High Plains during the summer of 1981 in connection with two neighboring projects. The radar data were collected at Bowman, North Dakota, as part of the North Dakota Cloud Modification Project (NDCMP), and at Miles City, Montana, as part of the Cooperative Convective Precipitation Experiment (CCOPE). Descriptions of these activities appear in Miller et al. (1983) and Knight (1982), respectively.

a. Database and analysis procedure

Doneaud et al. (1987) describe the general analysis procedure and provide detailed examples. Data were recorded by a C-band radar with a 2° beamwidth at Bowman and another C-band radar with a 1° beamwidth at Miles City. The analyzed radar range was restricted from 20 to 150 km; the "low-tilt" data were defined as the 3° elevation PPI (plan position indicator) out to range 50 km and the 1° PPI beyond that range. The reflectivity values were converted from spherical to rectangular coordinates for display, and individual radar echo clusters were identified and tracked in successive scans. A radar "sector of interest," which enclosed each identified echo cluster, was defined for each low-tilt scan throughout the cluster lifetime. From the radar data at these low-elevation angles, estimates were calculated of the rain volume produced by each convective cluster, using an optimized Z–R relationship (Smith et al. 1975). This provides the "ground-truth" data for the ATI comparisons.

Echo areas within the 25-dBZ reflectivity threshold on each scan were also determined, for a parallel calculation of the corresponding radar ATIs. These areas, multiplied by the centered time interval between scans and summed over the lifetime of the cluster, produced the radar ATI values. The estimates of cluster rainfall volumes calculated from the radar data exhibit a strong correlation with these radar ATI values, which has already been documented (Doneaud et al. 1984b; Johnson and Hjelmfelt 1990).

The satellite rapid-scan data for the cases analyzed were reviewed to match as closely as possible the satellite image times to the radar scan times. All images were provided by GOES-West except for four that were

taken from GOES-East. (The data from GOES-East were included to reduce the size of the time step so that evolution of the particular cloud clusters could be followed more precisely.) Images were remapped from the satellite coordinate system to a Lambert conformal projection such that the meridional and zonal dimensions of an image pixel were nearly equal. Remapped imagery had a resultant areal resolution of 2.47 km^2 per image pixel.

The radar sector of interest was used to locate the convective cluster responsible for the rainfall in the remapped satellite data. A corresponding satellite sector of interest was then defined for detailed analysis by applying small adjustments to the radar sector using a manual processing technique. A total of 18 clusters, each lasting from 1 to 5 h, was identified for which both digital satellite and radar data existed. The area enclosed by each brightness level on each image was multiplied by the time interval between images, and the area–time products were summed over the lifetime of the cluster to produce an SATI value for each event and brightness level. The SATI values computed for each cluster varied as a function of the threshold brightness level because the horizontal extent of the cloud increases as brightness decreases (cloud-top temperature increases) in the IR images.

The uncertainties in the satellite data are twofold: first, there are physical errors due to view angle, and second, there are calibration problems. The view-angle error can be corrected and the calibration error is not significant for this analysis. A calibration error will affect the entire range of brightness temperatures in a manner that preserves the relative gradient of brightness while shifting the absolute temperature scale. Calculation of a satellite ATI value for each brightness level preserves the variations as long as the sensor calibration is stable over the duration of the storm; in this study, the maximum storm duration was 10 h. The temperature values are provided mainly for convenience and are not essential to the calculation.

An optimization scheme was developed to determine the digital brightness-count threshold that would yield satellite area–time integrals that would be most closely related to the radar-estimated rainfall values for the clusters. To determine this optimized threshold, a regression analysis correlated the calculated SATIs for each specific brightness level to the estimated rainfall volumes for the corresponding events. This operation yielded a correlation coefficient for each brightness level. In a somewhat similar analysis using the GARP (Global Atmospheric Research Program) Atlantic Tropical Experiment (GATE) data, Arkin (1979) found a rather broad maximum in the correlation coefficient. Moreover, in our analysis, the correlation could be affected by the number of events included (which increased as the brightness threshold decreased and more, smaller clusters were incorporated). The resulting correlation coefficient was therefore weighted by the number of events included in the regression to produce an optimization parameter. The weighting factor guarded against the possibility that a high correlation based on just a few events would unduly influence the optimization.

b. Results

Figure 1 demonstrates the results of the optimization procedure, with the brightness-level threshold converted to the corresponding infrared temperature. For each brightness level (IR temperature), the optimization parameter plotted on the ordinate is the product of the correlation coefficient r and the number of clusters N involved in the regression. With an IR threshold temperature of −22.5°C (or 251 K), the optimization parameter reaches a maximum. Thus, an optimized fixed threshold of −22.5°C provides SATI values that are most closely related to the rainfall for 17 events. An 18th cluster was analyzed but is not included here because the maximum cloud height did not exceed the −18.5°C level, and the SATI for a −22.5°C threshold is therefore undefined.

Figure 2 compares the satellite ATIs for this IR temperature threshold to the associated radar-estimated rain volumes. The correlation coefficient for the 17 cases is 0.93, which is significant but somewhat reduced from that typically found with radar-determined ATIs. The logarithmic standard error of estimate is 0.304, suggesting an uncertainty of about a factor of 2 (comparable to that found in standard radar Z–R estimates of rainfall). Unlike the radar ATI results, how-

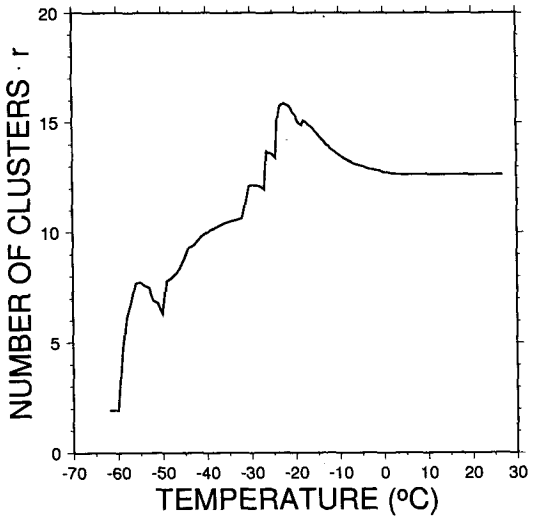

FIG. 1. Illustration of the results of the optimization procedure for northern High Plains data. To obtain the optimization parameter plotted on the ordinate for each brightness threshold, given here as the corresponding IR temperature, a correlation coefficient from the log–log regression of radar-estimated rain volume upon satellite ATI is multiplied by the number of clusters with a cloud-top temperature equal to or lower than the threshold temperature.

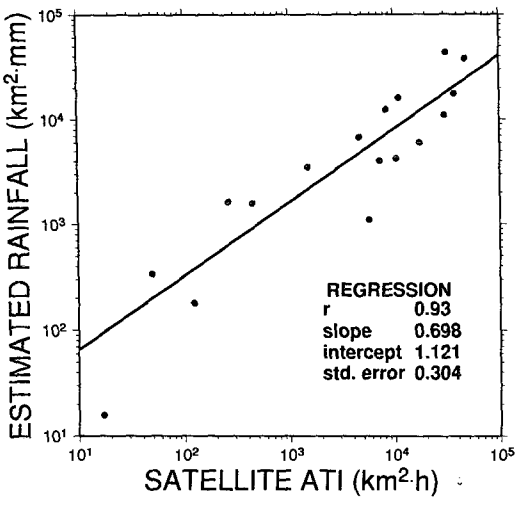

FIG. 2. Scatterplot and linear regression of radar-estimated rainfall versus satellite ATI for the infrared temperature threshold of −22.5°C. The regression line provides a calibration to convert satellite ATI values to rainfall estimates.

ever, the slope of 0.698 on the log–log plot is substantially less than unity. (In fact, only for threshold temperatures higher than −20°C did the regression slope even approach unity.) This indicates that the area and/or duration of the −22.5°C cloud shield increases more rapidly with cluster "size" than does the rain volume produced by the cluster.

Comparison with the corresponding radar ATIs (as in Atlas and Bell 1992) shows that the SATI based on the −22.5°C threshold tends to be representative of the raining portion of the cloud for small events (rain volumes in the neighborhood of 200 km^2 mm). For larger storms that produce up to 10^5 km^2 mm rainfall, the SATI determined by this threshold is much larger than the actual raining area indicated by radar. Thus, the satellite-determined SATI does not necessarily represent just the raining portion of the cluster; this conceptual requirement guided the selection of the threshold in some earlier radar ATI studies, but it is not essential as long as the interest is in total rain volume rather than its spatial or temporal distribution.

The GPI, in effect, assumes a slope of unity in the relation between rainfall and integrated cloud area. Atlas and Bell (1992) suggested that the behavior noted above may be the reason why the GPI can produce consistently accurate results only when area–time domains large enough to include a representative sample of clusters are employed. The GPI uses a threshold temperature of 235 K (−38°C), some 16° lower than the threshold reported here; Table 1 presents regression results for both thresholds [along with ones for the +8.5°C threshold determined for the COHMEX (Cooperative Huntsville Meteorological Experiment) data in section 3]. With the GPI threshold applied to the High Plains data, the rain volume–SATI correlation decreases to 0.79 and the regression slope to 0.449. On the other hand, the standard error of estimate becomes somewhat smaller.

A satellite ATI calculation based upon use of a fixed IR temperature threshold (−22.5°C for this dataset) would lead to rainfall estimates totally derived from satellite data, once the relationship to rainfall volume has been calibrated. The correlation with rainfall demonstrated in Fig. 2 provides the kind of calibration necessary to make the SATI useful for this purpose.

3. Analysis of COHMEX data

The regression line in Fig. 2 could be used for future estimation of convective rainfall in southeast Montana and southwest North Dakota, but it would be useful to compare it to independent data as well to determine whether a similar relationship applies in other climatological regimes. The scarcity of available radar and rapid-scan satellite data in a continuously recorded format limits the opportunities for the former, but data from the southeastern United States are available for the latter. Data collected during the 1986 COHMEX project centered at Huntsville, Alabama (Dodge et al. 1986), included simultaneous rapid-scan satellite and continuous volume-scan radar data.

a. Analysis and results

The National Weather Service RADAP (WSR-57 radar data processor) radar station located at Nashville, Tennessee, completed a volume scan every 10 min. The data from the S-band radar with a 2° beamwidth were recorded out to a range of 235 km. The general analysis procedure was the same as that outlined in section 2a. Radar estimates of rainfall volumes for individual echo clusters were calculated using a Z–R relationship appropriate for the southeastern region (Peterson et al. 1990). Also, the parallel calculation of radar ATI values was repeated for these data. Further details of the radar analysis appear in the Appendix.

Of the 287 echo clusters whose history was followed in the radar data, only 85 could be isolated, correlated with cloud clusters, and followed in the satellite infrared data. For each of those 85 clusters, the infrared cloud-top area was computed for each brightness threshold on each scan throughout the lifetime of the event. An SATI was then computed for each cluster with each IR threshold, and the same optimization scheme described in section 2a was applied to this dataset.

The results of the optimization for the COHMEX data are presented in Fig. 3, which shows the optimization parameter as a function of the IR temperature threshold. Much of the increase in the ordinate, from very low threshold temperatures, is due to the increase in the number of smaller clouds included rather than to any substantial variation in the correlation coefficient.

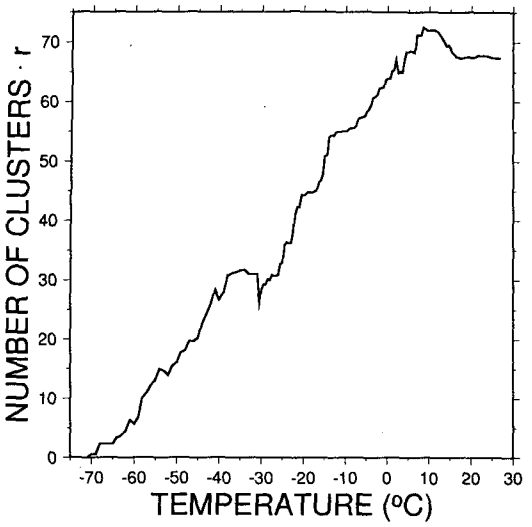

FIG. 3. Plot of the optimization parameter (as in Fig. 1) versus threshold temperature for COHMEX data.

The peak is much less pronounced in this case, but the procedure did optimize at a threshold temperature of 8.5°C (or 282 K). All 85 clusters were included at this stage of the optimization.

The optimum threshold temperature is 31°C higher for the COHMEX clouds, a fact presumably related to the difference in the dominant precipitation mechanisms in the southeastern United States as compared to those in the High Plains. In the southeast, rain reaches the ground from many clouds of modest depth due to warm-rain processes that are generally absent in the northern plains. Additionally, less precipitation is lost due to evaporation because there is usually a more moist environment below cloud base. More surprisingly, the optimum threshold is 47°C higher than that used in the GPI calculations; the GPI threshold was determined from data from the GATE region, where one would expect precipitation processes more nearly like those in the southeastern United States. The higher threshold temperature results in the inclusion of most of the cloud area in the SATI calculation. As a consequence, the SATI for a given cluster is usually considerably larger than the corresponding radar ATI. The rain volume–ATI regression lines based on radar and satellite ATI values therefore do not intersect within the range of these observations.

The comparison of the resultant satellite ATI values to radar-estimated rainfall volumes is demonstrated in Fig. 4. The COHMEX clusters tend to yield less rainfall than High Plains clusters with similar SATI values, a fact presumably related to the greater cloud area encompassed by the higher IR temperature threshold used in the COHMEX calculations. The correlation coefficient for this regression (0.85) is somewhat lower than that determined for the High Plains cases, and the logarithmic standard error of estimate (0.383) is a little higher. The regression line in this comparison has a slope of 0.818, which is slightly greater but still significantly less than unity. Once again the regression slope would only approach unity for high threshold temperatures, here greater than 10°C.

Table 1 summarizes a number of the regression relationships, for both the High Plains and the COHMEX datasets. To facilitate comparisons, the table provides results for each dataset using 1) its optimum threshold temperature, −22.5°C or +8.5°C, respectively; 2) the optimum threshold determined for the other dataset; and 3) the −38°C (235 K) threshold used for the calculations of the GPI. With the GPI threshold applied to the COHMEX data, the correlation drops to 0.63 and the slope to 0.371, while the standard error increases to 0.425. For the COHMEX data, the last two rows include some regression results based on subdivisions of the data as discussed in the next subsection.

b. Discussion

The correlation of 0.85 found in the COHMEX dataset is significant and corresponds to similar values reported by Arkin (1979) and others. Thus, a fixed-threshold satellite ATI analysis for all events in the southeastern United States appears to provide a useful correlation with rainfall estimates. However, the suggested thresholds are vastly different for the datasets from the two different regions, and there is greater scatter than in the corresponding results for the northern plains. The reasons for this are worth exploring.

From Fig. 4, it is evident that cluster rainfall amounts varied over more than three orders of magnitude, while according to Table 1, the cloud-top temperatures were distributed over an 81° range. Some clusters experienced dynamic growth and reached quite low cloud-

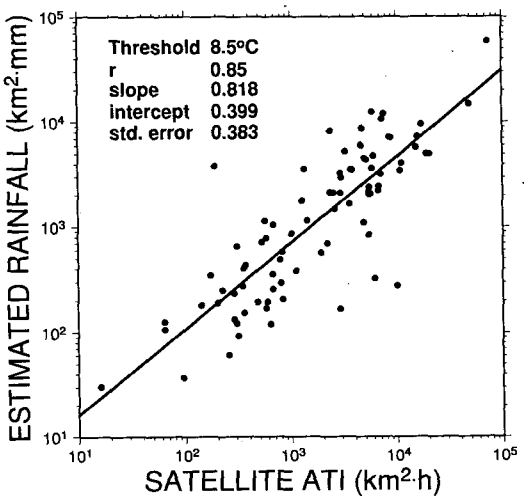

FIG. 4. Scatterplot and linear regression of radar-estimated rain volume versus satellite area–time integral for the threshold temperature of 8.5°C.

TABLE 1. Summary of regression results.

log(RERV) vs log(SATI) least-squares regression							
Cloud-top temperature range (°C)	No. of clusters	Optimization parameter	IR threshold (°C)	Correlation coefficient	Slope	Intercept	Standard error
High Plains							
−62 to −18.5	18	13	8.5	0.70	0.904	−0.054	0.591
−62 to −22.5	17	16	−22.5	0.93	0.698	1.121	0.304
−62 to −38	13	10	−38.0	0.79	0.449	2.272	0.273
COHMEX							
−72 to +8.5	85	72	8.5	0.85	0.818	0.399	0.383
−72 to −22.5	57	38	−22.5	0.67	0.447	2.059	0.440
−72 to −38	49	31	−38.0	0.63	0.371	2.425	0.425
−72 to −38	49	35	5.0	0.71	0.744	0.736	0.388
−31 to +8.5	35	26	8.5	0.74	0.816	0.379	0.370

top temperatures, while others remained shallow. This would suggest that many of the events involved an ice process, while only the warm-rain process was operative in others. The difference may be related to whether or not raindrops formed in a vigorous updraft where they could later be carried aloft and freeze to release latent heat; the released energy would then invigorate the cloud's vertical development.

This suggests the possibility of a bimodal, or at least a broader, distribution related to the different precipitation mechanisms; the data were examined for evidence of this. Figure 5 presents the number of clusters with cloud-top temperatures that equal or exceed the value given on the abscissa. A definite break occurs between −30° and −40°C, so there appear to be two groups. It is interesting that the threshold used for the GPI, 235 K or −38°C, falls right in this gap. Thus it is possible that there are two distinct groups of convective clouds, with only a portion of the clouds having the energy necessary to penetrate above the −30°C level. The cold-topped group (more than half the clusters) experienced good vertical development, reaching the tropopause level. Further cloud development may have resulted in a dome whose horizontal cross-sectional area (and/or persistence) increased more rapidly with increasing height than was the case for the warm-topped clusters.

For the satellite-derived ATIs, it may therefore be more appropriate to subdivide the data using cloud-top height (or temperature) as the criterion. The COHMEX events were accordingly divided into two groups by splitting at the −35°C cloud-top temperature level. The

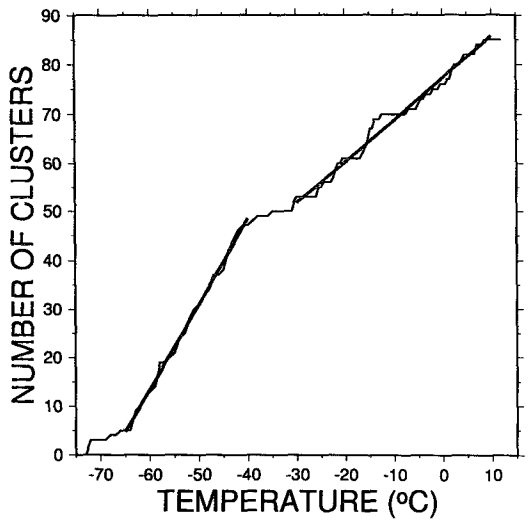

FIG. 5. Plot of the number of clusters with a cloud-top temperature less than or equal to the abscissa temperature. The break in the relationship is quantized by the two straight lines determined by regression. Slopes of the two lines are 1.75 (cold clouds) and 0.85 (warm clouds).

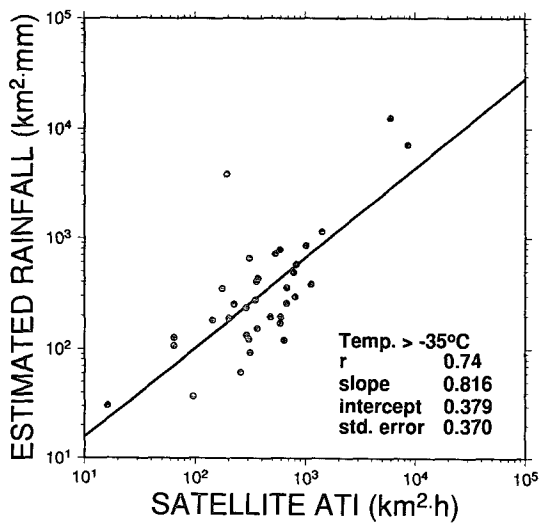

FIG. 6. Scatterplot and linear regression for radar-estimated rain volume versus satellite ATI for COHMEX clusters with cloud-top temperatures greater than −35°C.

optimization scheme was then applied separately to both subsets of data. The optimization for the "warm" subset, with cloud-top temperatures greater than −35°C, yielded an infrared temperature threshold of 8.5°C (the same as for the whole group). This subgroup includes the small rain producers; most of these events yielded less than 1000 km^2 mm rainfall. Figure 6 presents the comparison of the radar-estimated rainfalls for this subgroup versus the SATIs. The regression line is almost identical to that originally obtained for the combined dataset, although, as indicated in Table 1, the correlation coefficient is somewhat lower. This may be due primarily to the effective reduction in the range of values included in this subset.

The same analysis was repeated on the subset of "cold" storms with cloud-top temperatures less than −35°C, and an optimized temperature threshold of 5°C was obtained. Figure 7 gives the comparison of the radar-estimated rainfalls to the satellite ATIs for this subgroup. The regression line here differs somewhat from that for the full dataset (Table 1); the lower correlation coefficient of 0.71 leads to a slightly lower slope, here 0.744. However, the regression lines and standard errors of estimate for the two subsets differ only slightly, so it must be concluded that this partitioning of the data did little to improve the comparison of the radar-estimated rainfall versus satellite ATI for the COHMEX clusters.

Subgrouping of the COHMEX data for these analyses was accomplished by a software alteration. This alteration provided a mechanism for testing other subgroupings as well, and some additional subgroupings based upon cloud-top temperature were investigated. However, none of these led to a clarification of the reasons for the apparent geographical differences in the optimized temperature threshold or the rain volume–SATI relationship.

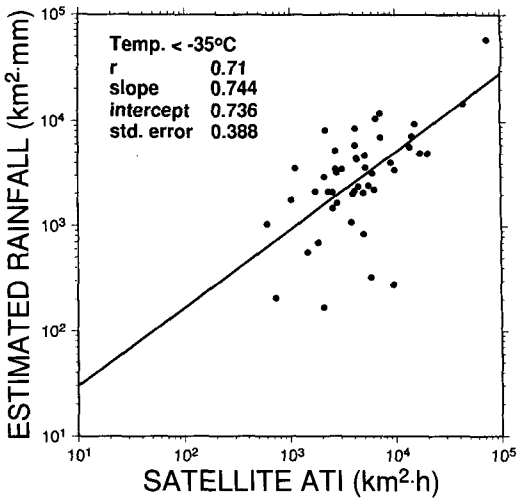

FIG. 7. Scatterplot and linear regression for radar-estimated rain volume versus satellite ATI for COHMEX clusters with cloud-top temperatures less than −35°C.

4. Conclusions

The relationship between convective rainfall volumes and satellite-derived ATIs based upon a fixed IR threshold (here found to be −22.5°C) appears to be fairly strong in the northern Great Plains. The rainfall-versus-SATI regression in Fig. 2 provides an initial calibration that could be used to convert satellite ATIs to estimates of rainfall for this region. Such estimates should, on the average, be within a factor of 2 of the actual rainfall, based upon the logarithmic standard error of 0.304. The fact that the slope of the log–log regression is considerably less than unity suggests that the cloud-top area and/or duration increases at a greater rate than the rainfall volume produced by a cloud cluster. Consequently, the average rainfall rate $\bar{R}$ for a cluster, which is the ratio of the rain volume to the ATI, varies appreciably with its "size." Thus, use of simple cloud-top area–time products with a mean rainfall rate assumed to be constant, as in the GOES precipitation index, may produce erroneous precipitation estimates unless the area–time domain considered is sufficiently large to ensure that a representative sample of clusters is included in the calculation. [Richards and Arkin (1981) noted that the simple linear relationship is limited to scales considerably larger than the convective scale, and Atlas and Bell (1992) also pointed out this condition.] The general tendency would be to overestimate rainfall from larger and longer-lived cloud clusters. The fact that the GPI works as well as it does may reflect a balance between overestimates due to this cause and underestimates due to omission of warm-topped clusters that do not reach the 235 K threshold.

Comparison of estimated rainfall to radar ATIs is more straightforward; the radar "sees" the precipitation more directly and cloud-top characteristics are not an issue. Moreover, the slopes of the rain volume–radar ATI relationships tend to be very close to unity. This means the average rainfall rates are more nearly independent of the echo-cluster "size," a fact that gives the radar ATIs (and the corresponding rain volumes) a convenient additive property not present in the satellite data.

The determination of a fixed IR-temperature threshold for calculating the SATIs in the southeastern region of the United States yields a much different result. The optimized threshold is 8.5°C, which results in the inclusion of most of the horizontal extent of the cloud in determining the SATI. The relationship to rain volume is again reasonably strong, and the regression slope is again substantially less than unity but, for these data, the standard error of estimate is somewhat greater. The regression line presented in Fig. 4 would be applicable to rainfall estimation based upon satellite-determined ATI values for this region.

The difference between the optimized thresholds for calculating the SATI values in the northern High Plains and the southeastern United States suggests an important geographic variation or perhaps one related to the basic precipitation process. A still different threshold, which was determined using GATE data from the tropical Atlantic, is used for the GPI. This indicates the possible need for a separate determination of the threshold and calibration of the relationship for each region of interest.

In light of these findings, an alternative SATI approach involving determination of an "adaptive" threshold is also being explored for more practical use in such things as developing global climatologies. A significant correlation exists between the minimum cloud-top temperature reached over the cluster lifetime and the infrared temperature threshold that would produce a satellite ATI for the cluster that matches the radar ATI in magnitude. The radar ATI is known to be closely correlated with the cluster rain volume, so such matching of the ATI values could lead to a similar correlation using the satellite-based ATIs. The cloud-top-temperature correlation may provide a plausible method for establishing the most appropriate IR temperature threshold for each cloud cluster. Doneaud et al. (1987) considered such an approach, and further work along this line will be reported in a future paper.

Acknowledgments. This research was sponsored by the National Aeronautics and Space Administration under Grant NAG 5-386; some of the early satellite data processing for this research was sponsored by the U.S. Army Research Office under Contract DALL03-86-K-0175 P00021. All figures were produced by GMT-SYSTEM version 2.0, which was provided by the University of Hawaii accessed through Internet.

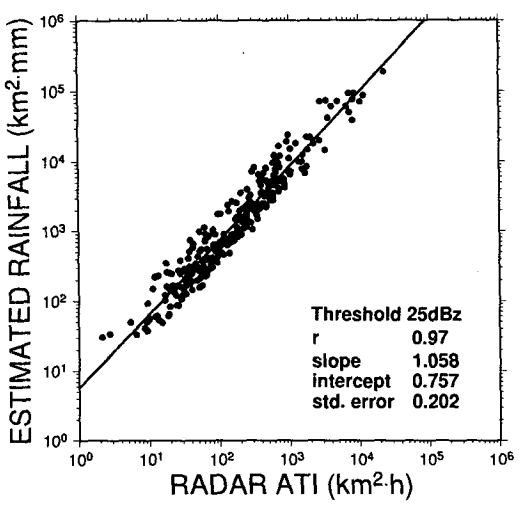

FIG. A1. Log–log scatterplot of radar-estimated rainfall versus radar area–time integral and regression line for 287 cloud clusters. Data collected by RADAP at Nashville during COHMEX.

TABLE A1. Parameters of rainfall–radar ATI relationships.

Project	Year	K	b	Radar Type	Radar Beamwidth
CCOPE	1981	2.12	1.09	C band	1°
NDCMP	1981	3.07	1.08	C band	2°
COHMEX	1986	5.71	1.06	S band	2°

APPENDIX

Rain Volume–Radar ATI Relationship for COHMEX Data

A 25-dBZ threshold was used to determine radar ATI values for the COHMEX data, to be consistent with the previous analyses of High Plains data (Doneaud et al. 1984b; Johnson and Hjelmfelt 1990). The comparison between radar-estimated rain volumes (based on an appropriate Z–R relationship) and radar ATI values for 287 echo clusters produced a correlation coefficient of 0.97, as demonstrated in Fig. A1. This is only slightly lower than that obtained for studies conducted in Montana (0.99), North Dakota (0.98), and Florida [0.92 in linear space, Lopez et al. (1989)], and the slope is again very close to unity. Some deterioration of the correlation might be expected because echoes that occurred near the maximum range of 235 km were included in this study, while a maximum range of 150 km was applied to previous datasets.

The linear regression of $\log(V)$ on $\log(\text{ATI})$ in Fig. A1 corresponds to a power-law relationship,

$$V = K(\text{ATI})^b, \qquad \text{(A1)}$$

which relates the rain volume V to the ATI. Here K and b are constants determined from the regression; b is the slope and K is the antilog of the intercept. Table A1 presents a comparison of parameters for the radar-estimated rain volume relationships to radar area–time integrals for COHMEX and North Dakota–Montana observations. The value of K approximates the mean rainfall rate, which is seen to be somewhat higher in the southeastern (COHMEX) region.

REFERENCES

Adler, R. F., and A. J. Negri, 1988: A satellite infrared technique to estimate tropical convective and stratiform rainfall. *J. Appl. Meteor.*, **27**, 30–51.

Arkin, P. A., 1979: The relationship between fractional coverage of high cloud and rainfall accumulations during GATE over the B-scale array. *Mon. Wea. Rev.*, **107**, 1382–1387.

——, and B. N. Meisner, 1987: The relationship between large-scale convective rainfall and cold cloud over the western hemisphere during 1982–84. *Mon. Wea. Rev.*, **115**, 51–74.

——, and P. E. Ardanuy, 1989: Estimating climatic-scale precipitation from space: A review. *J. Climate*, **2**, 1229–1238.

Atlas, D., and T. L. Bell, 1992: The relation of radar to cloud area–time integrals and implications for rain measurements from space. *Mon. Wea. Rev.*, **120**, 1997–2008.

——, D. Rosenfeld, and D. A. Short, 1990: The estimation of convective rainfall by area integrals. I: The theoretical and empirical basis. *J. Geophys. Res.*, **95,** 2153–2160.

Barrett, E. C., and D. W. Martin, 1981: *The Use of Satellite Data in Rainfall Monitoring.* Academic Press, 340 pp.

Byers, H. R., 1948: The use of radar in determining the amount of rain falling over a small area. *Trans. Amer. Geophys. Union,* **29,** 2, 187–196.

Dodge, J., J. Arnold, G. Wilson, J. Evans, and T. Fujita, 1986: The Cooperative Huntsville Meteorological Experiment (COHMEX). *Bull. Amer. Meteor. Soc.,* **67,** 417–419.

Doneaud, A. A., P. L. Smith, A. S. Dennis, and S. Sengupta, 1981: A simple method for estimating convective rain volume over an area. *Water Resour. Res.,* **17**(6), 1676–1682.

——, S. Ionescu-Niscov, and J. R. Miller, Jr., 1984a: Convective rain rates and their evolution during storms in a semi-arid climate. *Mon. Wea. Rev.,* **112,** 1602–1612.

——, ——, D. L. Priegnitz, and P. L. Smith, 1984b: The area–time integral as an indicator for convective rain volumes. *J. Climate Appl. Meteor.,* **23,** 555–561.

——, J. R. Miller, Jr., L. R. Johnson, T. H. Vonder Haar, and P. Laybe, 1987: The area–time-integral technique to estimate convective rain volumes over areas applied to satellite data—A preliminary investigation. *J. Climate Appl. Meteor.,* **26,** 156–169.

Griffith, C. G., W. L. Woodley, P. G. Grube, D. W. Martin, J. Stout, and D. N. Sikdar, 1978: Rain estimation from geosynchronous satellite imagery—Visible and infrared studies. *Mon. Wea. Rev.,* **106,** 1153–1171.

Johnson, L. R., and M. R. Hjelmfelt, 1990: A climatology of radar echo clusters over southeastern Montana. *J. Wea. Mod.,* **22,** 49–57.

Knight, C. A., 1982: The Cooperative Convective Precipitation Experiment (CCOPE), 18 May–7 August 1981. *Bull. Amer. Meteor. Soc.,* **63,** 386–398.

Lopez, R. E., D. Atlas, D. Rosenfeld, J. L. Thomas, D. O. Blanchard, and R. L. Holle, 1989: Estimation of rainfall using the radar echo area time integral. *J. Appl. Meteor.,* **28,** 1162–1175.

Miller, J. R., Jr., S. Ionescu-Niscov, D. L. Priegnitz, A. A. Doneaud, J. H. Hirsch, and P. L. Smith, 1983: Development of physical evaluation techniques for the North Dakota Cloud Modification Project. *J. Wea. Mod.,* **15,** 34–39.

Peterson, B. A., D. J. Musil, and P. L. Smith, 1990: Computerized reduction of airborne foil impactor data from COHMEX thunderstorms. Preprints, *1990 Conf. Cloud Physics,* San Francisco, CA, Amer. Meteor. Soc., 352–355.

Richards, F., and P. Arkin, 1981: On the relationship between satellite-observed cloud cover and precipitation. *Mon. Wea. Rev.,* **109,** 1081–1093.

Scofield, R. A., 1987: The NESDIS operational convective precipitation estimation technique. *Mon. Wea. Rev.,* **115,** 1773–1792.

Smith, P. L., Jr., D. E. Cain, and A. S. Dennis, 1975: Derivation of an R–Z relationship by computer optimization and its use in measuring daily areal rainfall. Preprints, *16th Radar Meteorology Conf.,* Houston, TX, Amer. Meteor. Soc., 461–466.

Stout, J. E., D. W. Martin, and D. N. Sikdar, 1979: Estimating GATE rainfall with geosynchronous satellite images. *Mon. Wea. Rev.,* **107,** 585–598.

Tsonis, A. A., 1988: Single thresholding and rain area delineation from satellite imagery. *J. Appl. Meteor.,* **27,** 1302–1306.